Comparison of mathematical tumor growth models

Johanna Sápi*, Dániel András Drexler**, Levente Kovács*
*Research and Innovation Center of Óbuda University, Physiological Controls Group,
Óbuda University, Budapest, Hungary
Email: {sapi.johanna, kovacs.levente}@nik.uni-obuda.hu
**Department of Control Engineering and Information Technology,
Budapest University of Technology and Economics, Budapest, Hungary
Email: drexler@iit.bme.hu

***Abstract*—Tumor cells need a set of functional capabilities for development and growth. One of these capabilities is angiogenesis; tumor cells have to become able to force new vessel formation to ensure oxygen and nutrient supply. In the literature, there are several different growth models which aim to describe the growth characteristics. The model creation is a trade-off problem. On the one hand, the model has to be sufficiently complex to describe all the important processes which take part in the system; however, on the other hand, the model has to be sufficiently simple and manageable for real-life usability and – taking into account the applicability of biomedical control theory – for controller design. We discuss some relevant tumor growth models used in the literature showing their complexity and their modeling power.**

I. INTRODUCTION

Tumor growth is a very complex process and requires a complex system which contains several key points. Hanahan and Weinberg [1] have collected the set of functional capabilities which are necessary for tumors during their development; they labeled these capabilities as the "hallmarks of cancer" (Fig. 1):

- self-sufficiency in growth signals
- insensitivity to anti-growth signals
- evading apoptosis
- limitless replicative potential
- sustained angiogenesis
- tissue invasion and metastasis

One of these key capabilities is angiogenesis, the process of new vessel formation. Three main classes of mathematical models have been created in the field of antiangiogenic therapy [2, 3]:

- temporal models [4, 5];
- spatiotemporal models [6, 7];
- multiscale models [8, 9].

The main disadvantage of these models is that they are mechanistic or semi-mechanistic [10] models built up from physical equations, and they have not been validated with in vivo data in most of the cases. Exceptions (validated models) exist, however they have other problem. The Hahnfeldt model [4] is not valid any more in the light of new medical results. A newly created and validated model posed by Gevertz [8] takes into account numerous effects and as a result it is overly difficult (it has 13 variables and 21 parameters).

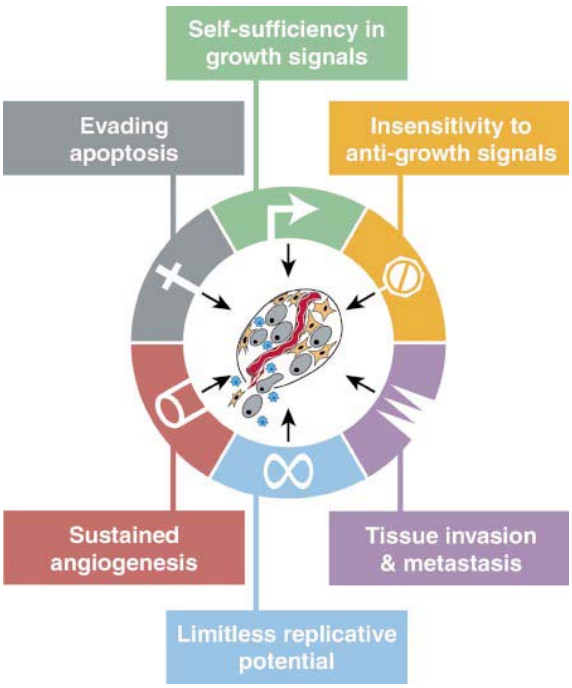

Figure 1. Hallmarks of cancer [1].

The paper gives a systematic overview of the different effects taken into account in the literature and is organized as follows.

In Section II, we review the linear-exponential growth models, from the simplest exponential model to a complex one which contains exponential and linear phases as well by taking into account the phenomenon of angiogenesis.

In Section III, we discuss the sigmoid shaped models like logistic and Gompertz models, together with a model, which assumes dynamic (time-dependent) carrying capacity.

In Section IV, a tumor growth model is presented in detail, in which the apoptosis is taken into account as a volume loss mechanism of the solid tumor.

Section V summarizes the tumor growth model inducing angiogenesis. Finally, the paper ends with the conclusions.

978-1-4673-9388-1/15/$31.00©2015 IEEE

II. LINEAR-EXPONENTIAL MODELS

A. Exponential growth model

The simplest tumor growth model is an exponential one:

$$N(t) = N(0) \cdot e^{\lambda t} \tag{1}$$

where *N(t)* is the current tumor size, *N(0)* is the initial tumor size, and λ is the growth parameter, which describes the speed of the growth.

B. Linear-exponential growth models

Several research articles [11, 12, 13] describe the phenomenon that tumor growth dynamics contains different phases, which can be described in a linear and exponential way.

Simeoni et al. [11] present a *minimal pharmacokinetic-pharmacodynamic model*, which describes the tumor growth in nontreated animals. They have found that the initial exponential phase is followed by a linear phase. In the study, a transit compartmental system was used to model the process of cell death at the later phase. The growth rate, which describes the above mentioned characteristics, can be formulated as a Cauchy problem [12]:

$$\begin{cases} \dfrac{dV}{dt} = a_0 V & t \le \tau \\ \dfrac{dV}{dt} = a_1 & t > \tau, \\ V(t=0) = V_0 \end{cases} \tag{2}$$

where a_0 belongs to the exponential phase, it is the coefficient of proliferative cells times $ln\ 2/T_C$ (T_C is cell cycle length); while a_1 is the coefficient of linear phase. From Equation (2), one can determine the value of τ:

$$\tau = \frac{1}{a_0} \log\left(\frac{a_1}{a_0 V_0}\right). \tag{3}$$

Tang et al. [13] modeled the three-dimensional tumor growth and angiogenesis to simulate tumor progression for chemotherapy evaluation. The whole complex model consists of three different levels: cellular, intratumora, and tissue level. The model defines the avascular tumor pressure, and the evolution of oxygen and carbon dioxide concentration for the *solid tumor growth model*. The *solid tumor angiogenesis model* takes into account the process of hypoxia, which is a frequent phenomenon in tumor cells in the lack of oxygen. The response of tumor cells to hypoxia is the secretion of tumor angiogenesis factors (e.g. vascular endothelial growth factor, VEGF). The process when the tumor becomes able to produce angiogenesis factors is called as angiogenic switch, since thereby the tumor will possess own blood vessels. In the model, tumor vessel growth is determined by the density of the angiogenesis factors and tumor interstitial pressure. The model secludes four different phases of the growth process (Fig. 2):

- exponential growth (*T1*),
- linear expansion (*T2*),
- stasis (*T3*),
- secondary growth (*T4*).

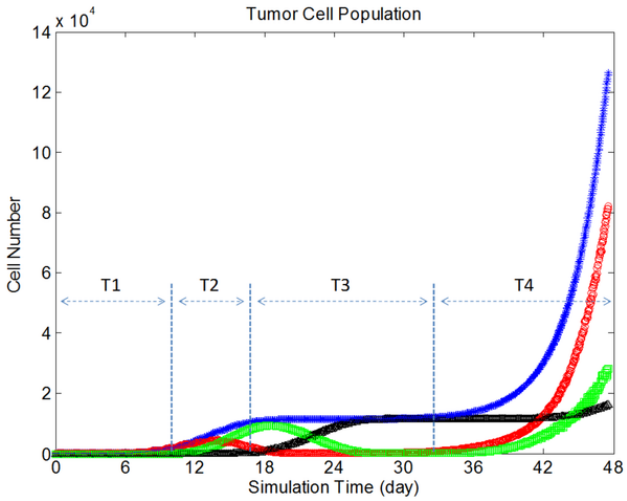

Figure 2. Tumor cell number over time. Blue: total cells; Red: active tumor cells; Green: quiescent tumor cells; Black: necrotic tumor cells. [13]

In *T1* an *T2* phases, the tumor is an avascular nodule. During phase *T1*, there are enough oxygen and nutrients for tumor growth; hence the growth characteristic is exponential. Due to the decreased level of oxygen, in phase *T2*, the growth rate slows down, resulting in a linear expansion. Phase *T3* represents a steady state of the tumor, in that phase, necrosis starts in the core of the nodule. Phase *T3* turns to *T4* when angiogenic switch occurs, *T4* results in a secondary, fast growth.

III. SIGMOID SHAPED MODELS (BASED ON THE CARRYING CAPACITY)

A. Logistic and Gompertz models

Several studies have shown that tumor growth has a sigmoid shape [12, 14, 15], viz. the growth function has an inflection point. After this point, the growth slows down in time and converges to a plateau. These types of models are based on the observation that the carrying capacity of the vessels has a maximal value.

The *logistic model* is defined by the following equations [12, 14]

$$\begin{cases} \dfrac{dV}{dt} = aV\left(1 - \dfrac{V}{K}\right) \\ V(t=0) = 1\,\mathrm{mm}^3, \end{cases} \tag{4}$$

where *a* is the coefficient of cell proliferation, and *K* is the carrying capacity.

The *Gompertz model* [12, 15] is described as

$$\begin{cases} \dfrac{dV}{dt} = ae^{-\beta t} V \\ V(t=0) = 1\,\mathrm{mm}^3, \end{cases} \tag{5}$$

where *a* is the coefficient of the initial proliferation rate, and β is the coefficient of growth deceleration. The solution of the Gompertz model is

$$V(t) = V_0 e^{\frac{a}{\beta}\left(1 - e^{-\beta t}\right)} \tag{6}$$

where $K = V_0 e^{\frac{a}{\beta}}$ is the carrying capacity.

B. *Dynamic carrying capacity based models*

Assuming a dynamic (time-dependent) carrying capacity, the following equations can be written [12]

$$\begin{cases} \dfrac{dV}{dt} = aV\log\left(\dfrac{K}{V}\right) \\ \dfrac{dK}{dt} = bV^{\frac{2}{3}} \\ V(t=0) = 1\,\text{mm}^3,\ K(t=0) = K_0, \end{cases} \tag{7}$$

where a and b are coefficients, and K is the carrying capacity.

The advantage of this type of model is that it can represent the vasculature as a limit of tumor growth [4].

IV. APOPTOSIS BASED TUMOR GROWTH MODEL (VOLUME LOSS OF THE SOLID TUMOR)

A. *The tumor growth model*

The tumor growth model, in which the apoptosis is taken into account as a volume loss mechanism of the solid tumor was created by McElwain and Morris [16]. The model assumes that the tumor is spherical.

In the model, the diffusion of nutrient is given by

$$\frac{k}{r^2}\frac{d}{dr}\left(r^2\frac{d\sigma}{dr}\right), \tag{8}$$

where k is the coefficient of nutrient diffusion, r is the current radius of the nodule, and σ is the local nutrient concentration.

The nutrient consumption ($Af(\sigma)$) and the proliferation ($sf(\sigma)$) are described as a function of the local nutrient concentration. Three different cases can be separated based on the current value of $f(\sigma)$

$$f(\sigma) = \begin{cases} 1 & \sigma^* \le \sigma \quad \rightarrow Case1 \\ \dfrac{\sigma}{\sigma^*} & \sigma_i < \sigma \le \sigma^* \quad \rightarrow Case2 \\ 0 & \sigma \le \sigma_i \quad \rightarrow Case3 \end{cases} \tag{9}$$

where σ^* is the critical level: cancer cells die when the nutrient concentration falls below this level.

In *Case1*, the proliferation and nutrient consumption are "normal" (the proliferation rate and the nutrient consumption rate are not weighted).

In *Case2*, "nutrient deficiency phenomena" occurs (the proliferation rate and the nutrient consumption rate decreases as linear functions of the current concentration level of nutrient).

In *Case3*, the tumor cells die and form a "coagulative necrotic core" (the proliferation rate and the nutrient consumption rate are zero).

B. *Phase I*

In Phase I, there are sufficient oxygen and nutrients for the tumor cells; hence the tumor growth is not limited, it shows an exponential growth characteristics. Cell proliferation occurs with normal growth rate (*Case1*), and apoptosis is active as well (Fig. 3).

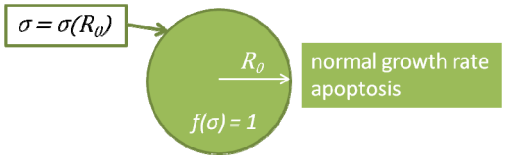

Figure 3. Phase I in the apoptosis based tumor growth model.

The diffusion of nutrient in this phase can be described as

$$\frac{k}{r^2}\frac{d}{dr}\left[r^2\frac{d\sigma}{dr}\right] = A, \quad 0 \le r \le R_0, \tag{10}$$

where A is the normal nutrient consumption rate, and R_0 is the outer radius of the nodule. Hence, the nutrient concentration as a function of the radius can be expressed as

$$\sigma(r) = \sigma(R_0) - \frac{A}{6k}\left(R_0^2 - r^2\right). \tag{11}$$

Taking into account that the change of the tumor volume depends on the difference of the growth and death rate, one can describe that

$$\frac{dV}{dt} = (s-\lambda)V, \tag{12}$$

where s is the normal local proliferation rate (growth rate), and λ is the local rate of volume loss due to apoptosis per unit volume per unit time (death rate).

In this light, the tumor growth equation which describes the evolution of the outer radius of the nodule in time is

$$\frac{4\pi}{3}\frac{dR_0^3}{dt} = s\frac{4\pi}{3}R_0^3 - \lambda\frac{4\pi}{3}R_0^3, \tag{13}$$

Considering that Equation (12) has the solution in the following form

$$V = ce^{s-\lambda t}, \tag{14}$$

the solution of the tumor growth Equation (13) can be written as

$$\sqrt{\frac{A}{k\sigma^*}}R_0(\tau) = \sqrt{\frac{A}{k\sigma^*}}R_0(0)e^{\frac{1}{3}(1-\gamma)\tau} \tag{15}$$

where $\tau = st$ is the scaled time, and $\gamma = \lambda/s$ (which has to be less than unity for the growth of the nodule).

This phase stops when the nutrient concentration at the center of the nodule becomes equal to the critical concentration ($\sigma(r = 0) = \sigma^*$). The value of the radius at which the tumor switches to Phase II becomes

$$R_0\,|_{pI\to pII} = \sqrt{\frac{6\left(\dfrac{\sigma(R_0)}{\sigma^*}\right)-1}{\dfrac{A}{k\sigma^*}}} \tag{16}$$

C. *Phase II*

In Phase II, a new layer appears in the tumor (Fig. 4). Beside the external region which has a normal growth rate (*Case1*), an inner nodule is developed which slows the growth rate (*Case2*) due to the nutrient and oxygen deficiencies.

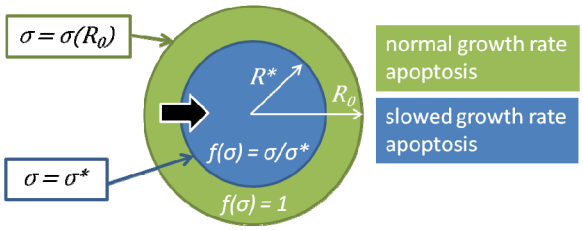

Figure 4. Phase II in the apoptosis based tumor growth model. The black arrow shows the cell migration from normal growth region to slowed growth region.

In this phase, the diffusion of the nutrient can be described as

$$\frac{k}{r^2}\frac{d}{dr}\left[r^2\frac{d\sigma}{dr}\right]=\begin{cases}A\dfrac{\sigma}{\sigma^*} & 0\le r\le R^*\\ A & R^*\le r\le R_0\end{cases}. \tag{17}$$

where $R^* = R(\sigma = \sigma^*)$.

The nutrient concentration when $0 \le r \le R^*$ is

$$\sigma(r)=\sigma^*\frac{R^*}{r}\frac{\sinh\left(\sqrt{\dfrac{A}{k\sigma^*}}r\right)}{\sinh\left(\sqrt{\dfrac{A}{k\sigma^*}}R^*\right)}, \tag{18}$$

while the nutrient concentration when $R^* \le r \le R_0$ can be expressed as

$$\sigma(r)=\sigma(R_0)+\frac{A}{6k}\left(r^2-R_0^2\right)+ \\ +\left(\sigma^*-\sigma(R_0)-\frac{A}{6k}\left(R^{*2}-R_0^2\right)\right)\left(\frac{R^*}{r}\frac{r-R_0}{R^*-R_0}\right). \tag{19}$$

The tumor growth equation can be described by

$$\frac{4\pi}{3}\frac{dR_0^3}{dt}=s\frac{4\pi}{3}\left(R_0^3-R^{*3}\right)-\lambda\frac{4\pi}{3}R_0^3+ \\ +4\pi s\int_0^{R^*}\frac{\sigma(r)}{\sigma^*}r^2dr, \tag{20}$$

and the solution of this growth function is

$$\frac{A}{k\sigma^*}R_0^2\frac{d\left(\sqrt{\dfrac{A}{k\sigma^*}}R_0\right)}{d\tau}=\frac{1}{3}(1-\gamma)\left(\sqrt{\frac{A}{k\sigma^*}}R_0\right)^3+ \\ +\left(\frac{\sigma(R_0)}{\sigma^*}-1-\frac{1}{6}\left(\frac{A}{k\sigma^*}R_0^2-\frac{A}{k\sigma^*}R^{*2}\right)\right)\frac{\dfrac{A}{k\sigma^*}R_0R^*}{\sqrt{\dfrac{A}{k\sigma^*}}(R_0-R^*)}. \tag{21}$$

The process of slowed growth can result in two different outcomes (Fig. 5). If the volume growth due to cell division is balanced by the volume loss due to apoptosis, a steady state (dormant state) can be attained. Otherwise, if at the center of the nodule the nutrient concentration becomes equal to σ_i, viz. $\sigma(r = 0) = \sigma_i$, a necrotic core formation will start and the tumor switches to Phase III.

D. *Phase III*

In Phase III, the tumor has a three layer structure (Fig. 6). In the outermost shell, there is a normal growth with exponential growth characteristics (*Case1*). In the middle shell, the growth is slowed due to nutrient deficiencies (*Case2*), while in the inner region tumor cells die and form a coagulative necrotic core (*Case3*).

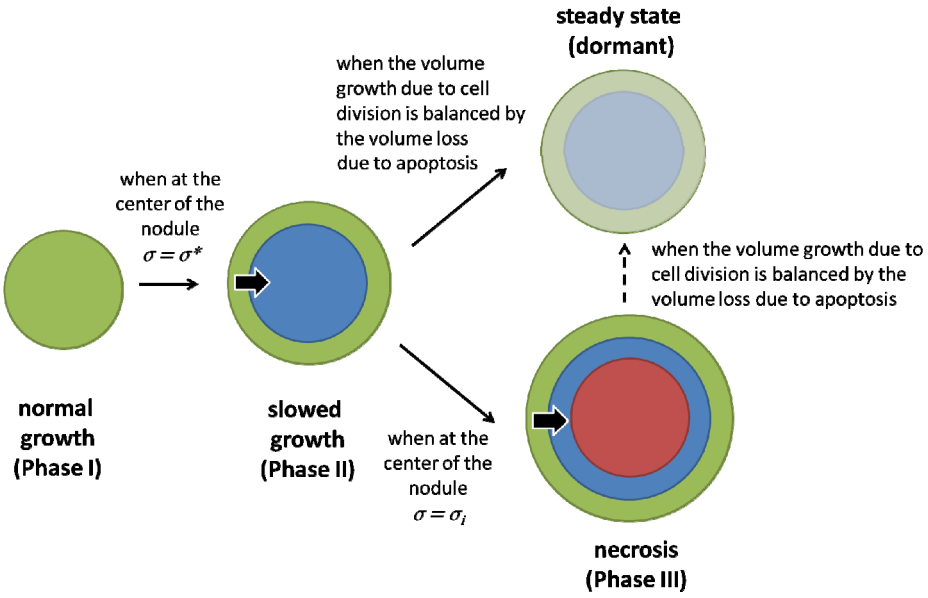

Figure 5. Summary of the processes which take part in the apoptosis based tumor growth model. The black arrow shows the cell migration from normal growth region to slowed growth region.

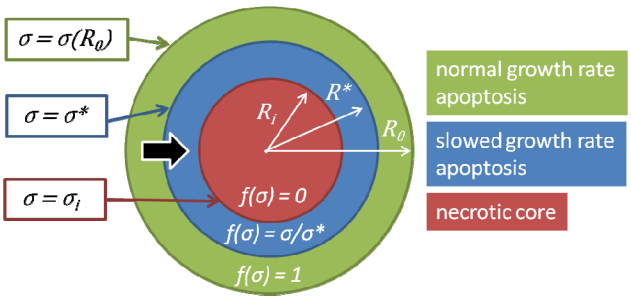

Figure 6. Phase III in the apoptosis based tumor growth model. The black arrow shows the cell migration from normal growth region to slowed growth region.

The diffusion of the nutrient in the three different regions is

$$\frac{k}{r^2}\frac{d}{dr}\left[r^2\frac{d\sigma}{dr}\right]=\begin{cases}0 & 0\le r\le R_i\\ A\dfrac{\sigma}{\sigma^*} & R_i\le r\le R^*,\\ A & R^*\le r\le R_0\end{cases} \tag{22}$$

where R_i, is the radius of the inner necrotic region.

The solution of the nutrient concentration when $0\le r\le R_i$ is

$$\sigma(r)=\sigma_i, \tag{23}$$

when $R_i\le r\le R^*$, the nutrient concentration becomes

$$\sigma(r)=\frac{\sigma_i}{\sqrt{\frac{A}{k\sigma^*}}r}\cdot \left[\sinh\left(\sqrt{\frac{A}{k\sigma^*}}(r-R_i)\right)+\sqrt{\frac{A}{k\sigma^*}}R_i\cosh\left(\sqrt{\frac{A}{k\sigma^*}}(r-R_i)\right)\right], \tag{24}$$

and finally, the nutrient concentration when $R^*\le r\le R_0$ results as

$$\sigma(r)=\sigma(R_0)+\frac{A}{6k}\left(r^2-R_0^2\right)+F\left(\frac{1}{R_0}-\frac{1}{r}\right), \tag{25}$$

where F causes σ to satisfy $\sigma(R^*)=\sigma^*$.

The tumor growth equation in Phase III is

$$\frac{4\pi}{3}\frac{dR_0^3}{dt}=s\frac{4\pi}{3}\left(R_0^3-R^{*3}\right)-\lambda\frac{4\pi}{3}\left(R_0^3-R_i^3\right)+ +4\pi s\int_{R_i}^{R^*}\frac{\sigma(r)}{\sigma^*}r^2dr, \tag{26}$$

and the solution of this growth function becomes

$$\left(\sqrt{\frac{A}{k\sigma^*}}R_0\right)^3\frac{d\left(\sqrt{\frac{A}{k\sigma^*}}R_0\right)}{d\tau}=\frac{1}{3}(1-\gamma)\left(\sqrt{\frac{A}{k\sigma^*}}R_0\right)^3+ +\frac{1}{3}\gamma\left(\sqrt{\frac{A}{k\sigma^*}}R_i\right)^3+ +\left(\frac{\sigma(R_0)}{\sigma^*}-1-\frac{1}{6}\left(\frac{A}{k\sigma^*}R_0^2-\frac{A}{k\sigma^*}R^{*2}\right)\right)\frac{\frac{A}{k\sigma^*}R_0R^*}{\sqrt{\frac{A}{k\sigma^*}}(R_0-R^*)}. \tag{27}$$

V. ANGIOGENESIS BASED TUMOR GROWTH MODEL

Yang [17] performed a mathematical model which describes the tumor growth inducing angiogenesis. The modeling concept was to describe an organ without tumor first, when normal cells and blood vessels are in a steady state; followed by the modeling of the organ with cancer cells.

The model discusses a pre-angiogenesis stage, where the cells are formed by the "mass action law" [18]. This stage is continued by the VEGF expression and finally the endothelial sprouting. The model assumes logistic growth for normal, cancer and epithelial cells as well.

The tumor growth model which takes into account angiogenesis, is described by the following system of equations

$$\frac{dC}{dt}=\alpha_1C\left[1-\frac{C}{k_1(E)}-\frac{\beta'_1T}{k_1(E)}\right]-\mu_1C-C_m\delta_D(t) \tag{28}$$

$$\frac{dE}{dt}=\alpha_2E\left[1-\frac{E}{k_2(C)}\right]-\gamma ET-\mu_2E \tag{29}$$

$$\frac{dT}{dt}=C_m\delta_D(t)+\alpha_3AT\left(1-\frac{T}{k_3}\right)+ +\alpha_3'T\left[1-\frac{T}{k_1(E)}-\frac{\beta'_2C}{k_1(E)}\right]-\mu_3T \tag{30}$$

$$\frac{dP}{dt}=\gamma ET-\delta P-\mu_4P \tag{31}$$

$$\frac{dA}{dt}=\delta P+\varepsilon TA\left(1-\frac{A}{k_4}\right)-\mu_5A \tag{32}$$

The equations contain the following parameters.

- C, E, T, P and A describe the concentration of normal, epithelial, cancer, pre-angiogenesis and angiogenesis cells, respectively.
- α_1, α_2, α_3 and ε mean the intrinsic growth rate of normal, epithelial, cancer and angiogenesis cells, respectively.
- μ_1, μ_2, μ_3, μ_4 and μ_5 denote the mortality rate of normal, epithelial, cancer, pre-angiogenesis and angiogenesis cells, respectively.
- k_1, k_2, k_3 and k_4 are the carrying capacity of normal, epithelial, cancer and angiogenesis cells, respectively.
- δ is the transfer rate from pre-angiogenesis to angiogenesis cells, and γ is the epithelial sprouting rate.
- β_1 describes the rate of inhibition of normal cells by cancer cells, and β_2 describes the rate of inhibition of cancer cells by normal cells.

VI. CONCLUSION

There is a strong need to create a mathematical model which describes the tumor growth dynamics under angiogenic inhibition. This model has to take into account the previously mentioned models and their results, but it has to be sufficiently simple to be manageable for both real-life applicability and controller design. Based on the supporting data of our research results we believe that such a model can be created [19-22].

REFERENCES

[1] D. Hanahan, R.A. Weinberg, "The hallmarks of cancer", *Cell*, vol. 100, no. 1, pp. 57-70, 2000.

[2] J. Mriouah, C. Boura, M. Thomassin, T. Bastogne, D. Dumas, B. Faivre, M. Barberi-Heyob, "Tumor vascular responses to antivascular and antiangiogenic strategies: looking for suitable models", *Trends Biotechnol*, vol. 30, no. 12, pp. 649-58, 2012.

[3] S.M. Peirce, "Computational and mathematical modeling of angiogenesis", *Microcirculation*, vol. 15, pp. 739-751, 2008.

[4] P. Hahnfeldt, D. Panigrahy, J. Folkman, and L. Hlatky, "Tumor development under angiogenic signaling: A dynamical theory of tumor growth, treatment response, and postvascular dormancy", *Cancer research*, vol. 59, pp. 4770–4775, 1999.

[5] A. D'Onofrio, A. Gandolfi, "A family of models of angiogenesis and anti-angiogenesis anti-cancer therapy", *Math Med Biol*, vol. 26, pp. 63-95, 2009.

[6] M.A. Chaplain, "Mathematical modelling of angiogenesis", *J. Neurooncol*, vol. 50, pp. 37-51, 2000.

[7] S.D. Finley, M.O. Engel-Stefanini, P.I. Imoukhuede, A.S. Popel, "Pharmacokinetics and pharmacodynamics of VEGF-neutralizing antibodies", *BMC Syst Biol*, vol. 21, pp. 193-213, 2011.

[8] J.L. Gevertz, "Computational modeling of tumor response to vascular-targeting therapies – part I: validation", *Comput Math Methods Med*, 2011, available: http://dx.doi.org/10.1155/2011/830515, accessed 01.07.2015.

[9] A. Stéphanou, S.R. McDougall, A.R.A Anderson, M.A.J. Chaplain, "Mathematical modelling of flow in 2D and 3D vascular networks: Applications to anti-angiogenic and chemotherapeutic drug strategies", *Math Comput Model*, vol. 41, pp. 1137-1156, 2005.

[10] B. Ribba, E. Watkin, M. Tod, P. Girard, E. Grenier, B. You, E. Giraudo, G. Freyer, "A model of vascular tumour growth in mice combining longitudinal tumour size data with histological biomarkers", *Eur J Cancer*, vol. 47, pp. 479-490, 2011.

[11] M. Simeoni, P. Magni, C. Cammia, G. De Nicolao, V. Croci, et al., "Predictive pharmacokinetic-pharmacodynamic modeling of tumor growth kinetics in xenograft models after administration of anticancer agents", *Cancer Res*, 2004, vol. 64, pp. 1094–1101, available: http://cancerres.aacrjournals.org/cgi/doi/10.1158/0008-5472.CAN-03-2524, accessed 01.07.2015.

[12] S. Benzekry, C. Lamont, A. Beheshti, A. Tracz, J.M. Ebos, L. Hlatky, P. Hahnfeldt, "Classical mathematical models for description and prediction of experimental tumor growth", *PLoS Comput Biol*, 10(8):e1003800. doi: 10.1371/journal.pcbi.1003800. eCollection 2014, available: http://journals.plos.org/ploscompbiol/article?id=10.1371/journal.pcbi.1003800#pcbi.1003800.e003, accessed 01.07.2015.

[13] L. Tang, A.L. van de Ven, D. Guo, V. Andasari, V. Cristini, K.C. Li, X. Zhou, "Computational modeling of 3D tumor growth and angiogenesis for chemotherapy evaluation", *PLoS One,* 9(1):e83962. doi: 10.1371/journal.pone.0083962. eCollection 2014, available: http://journals.plos.org/plosone/article?id=10.1371/journal.pone.0083962, accessed 01.07.2015.

[14] J.A. Spratt, D. von Fournier, J.S. Spratt, E.E. Weber, "Decelerating growth and human breast cancer", *Cancer*, vol. 71, no. 6, pp. 2013-2019, 1993.

[15] A. Akanuma, "Parameter analysis of Gompertzian function growth model in clinical tumors", *Eur J Cancer*, vol. 14, no. 6, pp. 681-618, 1978.

[16] D.L.S. McElwain, L.E. Morris, "Apoptosis as a Volume loss Mechanism in Mathematical Models of Solid Tumor Growth", *Mathematical Biosciences*, vol. 39. no. 1-2, pp. 147–157, 1978.

[17] H.M. Yang, "Mathematical modeling of solid cancer growth with angiogenesis", *Theor Biol Med Model*, vol. 9, no. 2, doi: 10.1186/1742-4682-9-2, 2012.

[18] L. Edelstein-Keshet, "Mathematical Models in Biology", New York: *McGraw Hill*, Inc; 1988.

[19] J. Sápi, D.A. Drexler, I. Harmati, A. Szeles, B. Kiss, Z. Sápi, L. Kovács, "Tumor growth model identification and analysis in case of C38 colon adenocarcinoma and B16 melanoma". *in Proc. 8th IEEE International Symposium on Applied Computational Intelligence and Informatics*, Timisoara, Romania, pp. 303-308, 2013.

[20] B. Kiss, J. Sápi, L. Kovács, "Imaging method for model-based control of tumor diseases", *in Proc. 11th IEEE International Symposium on Intelligent Systems and Informatics*, Subotica, Serbia, pp. 271-275, 2013.

[21] J. Sápi, D.A. Drexler, Z. Sápi, L. Kovács, "Identification of C38 colon adenocarcinoma growth under bevacizumab therapy and without therapy", *in Proc. 15th IEEE International Symposium on Computational Intelligence and Informatics*, Budapest, Hungary, pp. 443-448, 2014

[22] J. Sápi, L. Kovács, D.A. Drexler, P. Kocsis, D. Gajári, Z. Sápi, "Tumor Volume Estimation and Quasi-Continuous Administration for Most Effective Bevacizumab Therapy", Submitted to *Plos One*, 2015 January